

Study Of Microchannels With Fins For Effective Cooling Of Electronic Equipment With Help Of Cfd

¹Vishal S.Sanap, ²Dr. S.V. Dingare,

¹Student, M.E. Heat Power , ²Professor, Dept. of Mech. Engineering

^{1,2}MAEER'S MIT ,College Of Engineering, Kothrud, Pune

ABSTRACT

This paper includes Numerical study of different microchannel with internal fins to investigate fluid flow and heat transfer characteristics. Three types of microchannels are studied –square channel with conventional and cross fins and rectangular channel with conventional fins. Constant heat flux boundary conditions were assumed on external walls of microchannel along with mass flow inlet and atm pressure outlet condition. Result of average local nusselt no distribution along the channel length were obtained as function of the fin height ratio. The analysis was carried out for different fin height and flow parameters in presence of a hydrodynamically developed, thermally developing laminar flow. The existence of optimum fin height ratio for each type of microchannel is found out in present study.

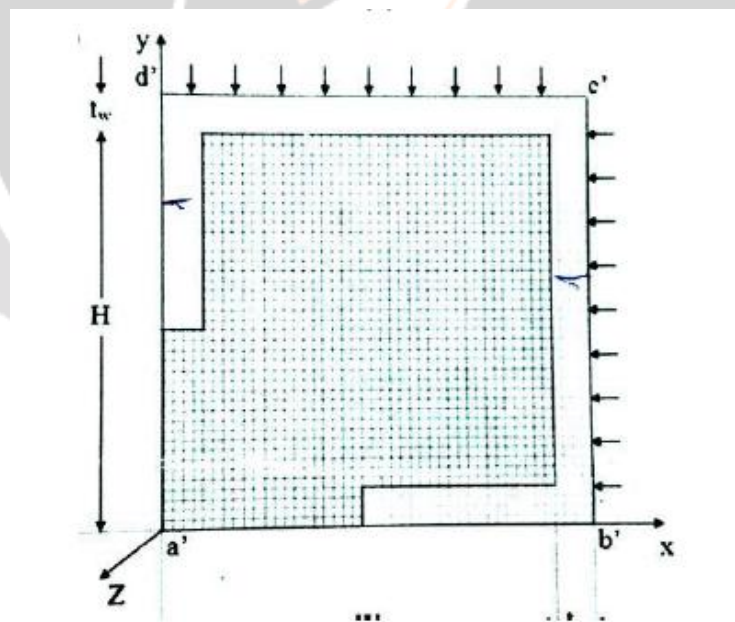
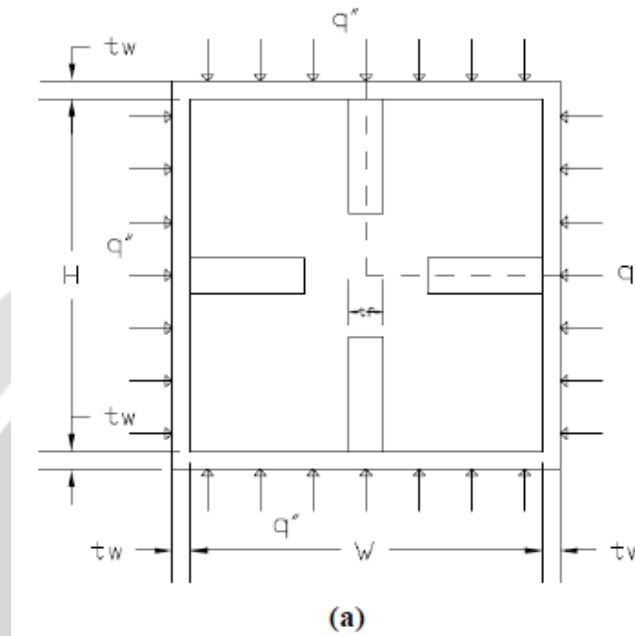
Keywords—; Microchannel; Electonic cooling; Heat flux; liquid cooling.

1. INTRODUCTION

In the natural system such as lungs and kidney in the human and other animals it has been observed that the transport processes become more efficient at microscale level dimensions. The increase in the area/volume ratio of passage and the change in the relative importance of different forces create new class of transport process that can lead to significant size reductions in practical devices utilizing this process. Although this benefits are well known as demonstrated by pioneering work of Tuckerman and Peace (1) significant research in this area started only after their successful application in high heat flux electronics cooling and microfluidic devices. The definition of microscale is somewhat flexible depending on dimension at which the transport characteristics are affected. In general channel dimension of 10-200 μ m are considered microscale. For improving operation reliability of electronic products efficient removal of internally generated heat is very important which also affect design consideration of microelectronic components. As many modern devices are densely packed with microelectronic circuit. Internal heat generated also increased and heat dissipation requirements have exponentially increased. So traditional cooling technique like fan cooling has become insufficient and imposes limits on product design. A significant amount of research has been made for developing some innovative cooling technique that have potential to deliver high heat flux rates for microelectronic application. The concept of microchannel can be best practical alternative for meeting the future cooling needs of advanced electronic

applications. The use of very large scale integrated (VLSI) electronic modern devices where internal heat generation has dramatically increased microchannel heat sink with passive enhancement devices find application in portable electronic equipment , miniature fuel cells etc and have become major focal point for challenging research activities in the field of heat transfer.

2. MODEL FORMULATION AND SOLUTION PROCEDURE :-



(b)

Fig.1.(a) Schematic diagram showing the cross section of square microchannel with conventional internal fins.(b) Computational domain and the grid pattern

The square channel is $200\ \mu\text{m}$ (W) \times $200\ \mu\text{m}$ (H) in crosssection, and $120\ \text{mm}$ (L) in length and rectangular channel is $400\ \mu\text{m}$ (W) \times $200\ \mu\text{m}$ (H) in cross-section, and $120\ \text{mm}$ (L) in length . The microchannel and all the

internal fins are considered to be made of aluminium. Channel wall thickness (t_w) of 10 μm and fin thickness (t_f) of 20 μm are used in the study, and are kept constant. Fin height ratios H^* from 0 (nofin) to 0.9 were considered in the modeling

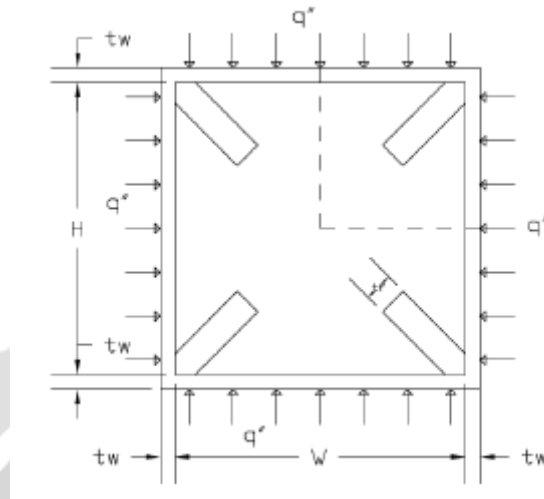


Fig.1(c) Schematic diagram showing the cross section of square microchannel with cross internal fins.

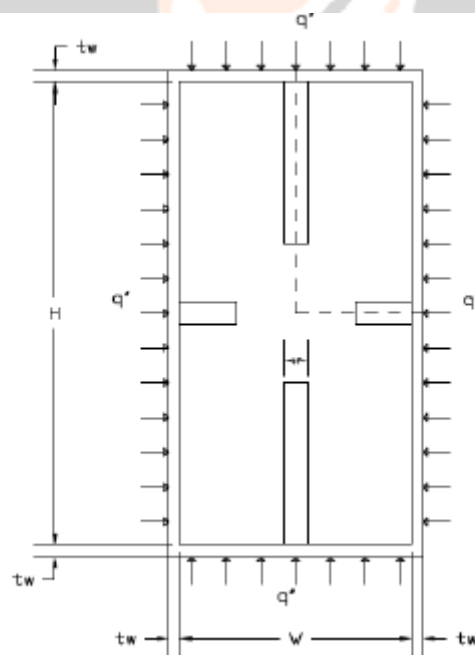


Fig.1.(d) Schematic diagram showing the cross section of rectangular microchannel with conventional internal fins

The dashed lines shown in Fig. 1(a) are the boundaries of the computational domain, where symmetrical boundary conditions are considered. The external walls of the channel are subjected to a uniform heat flux thermal boundary condition. A uniform heat flux of $5 \times 10^5 \text{ W/m}^2$ is applied at the four external walls of the

channel. Hydrodynamically fully developed laminar flow of water at an inlet temperature of 300 K is assumed to enter the channel. The flow is assumed to be steady, and undergoes thermal boundary layer development from the inlet of the channel. The microchannel is sufficiently long, such that both hydrodynamically and thermally fully developed flow is obtained at the channel outlet. The following boundary conditions are specified: atm pressure boundary condition at the channel and symmetrical boundary condition at the symmetrical wall. The symmetrical boundary condition reduces the number of nodes required for the model, and thus reduces the computational time and iteration for convergence. The symmetrical boundary condition assumes that no diffusion flux transfer occurs across the symmetry plane, and that the normal gradients of all flow variables are zero. The Reynolds number is suitably varied within the laminar region (1100—1330) with a constant mass flow rate of 2.2×10^{-4} kg/s for square channel and 4.4×10^{-4} kg/s for rectangular channel for all fin height ratios. Assuming steady, laminar and incompressible flow conditions together with the specified boundary conditions, the continuity, Navier-Stokes, and the energy equation were solved using the Finite volume based computational fluid dynamics solver FLUENT 6.3. The following governing equations were used in the mathematical modelling.

Continuity :

$$\frac{\partial \rho}{\partial t} + \nabla \cdot (\rho \mathbf{u}) = 0 \quad (\text{i})$$

Momentum :

$$\begin{aligned} \rho \left(u \frac{\partial u}{\partial x} + v \frac{\partial u}{\partial y} + w \frac{\partial u}{\partial z} \right) &= -\frac{\partial p}{\partial x} + \mu \left(\frac{\partial^2 u}{\partial x^2} + \frac{\partial^2 u}{\partial y^2} + \frac{\partial^2 u}{\partial z^2} \right) \\ \rho \left(u \frac{\partial v}{\partial x} + v \frac{\partial v}{\partial y} + w \frac{\partial v}{\partial z} \right) &= -\frac{\partial p}{\partial y} + \mu \left(\frac{\partial^2 v}{\partial x^2} + \frac{\partial^2 v}{\partial y^2} + \frac{\partial^2 v}{\partial z^2} \right) \\ \rho \left(u \frac{\partial w}{\partial x} + v \frac{\partial w}{\partial y} + w \frac{\partial w}{\partial z} \right) &= -\frac{\partial p}{\partial z} + \mu \left(\frac{\partial^2 w}{\partial x^2} + \frac{\partial^2 w}{\partial y^2} + \frac{\partial^2 w}{\partial z^2} \right) \end{aligned} \quad (\text{ii})$$

Energy equation for liquid :

$$\begin{aligned} \rho C_p \left(u \frac{\partial T}{\partial x} + v \frac{\partial T}{\partial y} + w \frac{\partial T}{\partial z} \right) &= K f \nabla^2 T + 2 \mu \left(\left(\frac{\partial u}{\partial x} \right)^2 + \right. \\ &\left. \left(\frac{\partial v}{\partial y} \right)^2 + \left(\frac{\partial w}{\partial z} \right)^2 \right) + \mu \left(\frac{\partial u}{\partial y} + \frac{\partial v}{\partial x} \right)^2 + \left(\frac{\partial u}{\partial z} + \frac{\partial w}{\partial x} \right)^2 + \\ &\left(\frac{\partial v}{\partial z} + \frac{\partial w}{\partial y} \right)^2 \end{aligned} \quad (\text{iii})$$

Energy equation for solid :

$$K_w \nabla^2 T = 0 \quad (\text{iv})$$

Fig.1(b) shows the computational domain and the grid pattern. For the sake of completeness, the boundary conditions corresponding to fig.1(b) are mathematically restated below

Symmetrical boundary conditions along a'b'

$$\frac{\partial w}{\partial y} = 0, \quad \frac{\partial T}{\partial y} = 0$$

Symmetrical boundary conditions along a'd'

$$\frac{\partial w}{\partial x} = 0, \quad \frac{\partial T}{\partial x} = 0$$

Constant heat flux wall boundary condition along b'c' and d'c'

$$q'' = 5 \times 10^5 \text{ W/m}^2$$

The SIMPLE algorithm was used to solve the pressure velocity coupling. The standard discretization scheme was used in the modelling following the first order upwind of the momentum and energy discretization. The convergence criterion that was used to ensure accuracy in the modelling is less than 10^{-6} for the scaled residues of mass and momentum flux. The average local Nusselt number and surface heat transfer coefficients were obtained from the numerical simulation once the convergence criterion was satisfied. The average local Nusselt number and the convective heat transfer coefficient on the inside walls of the channel are defined using the following equations.

$$Nu = \frac{hL}{K} = \frac{qDh}{K(T_w - T_b)} \quad (V)$$

In above Eqs T_w is the local average wall temperature, T_b is the local bulk fluid temperature. 2.1 Grid Independence : Grid independence test was conducted on the square unfinned channel to ensure that the obtained result does not depend on the meshing scheme followed. This involved meshing the same geometry of a square unfinned channel using three different grid sizes and comparing their results. Uniform hexahedral cells of $10 \times 10 \times 400$ (coarse), $20 \times 20 \times 400$ (medium) and $40 \times 40 \times 400$ (fine) were considered for the grid independence study. The local average Nusselts number at the exit for unfinned microchannel was obtained as 4.17, 4.05 and 4.03 respectively. Thus upon refinement from coarse to medium grid, an improvement of 2.87% was obtained and upon further refinement from medium to fine mesh only 0.49% improvement was obtained. The variation of average local Nusselts number with distance from the inlet of the channel obtained from the grid independence test for finless channels is shown in the fig 2. It can be seen from the graph that the variation of the results with alteration the grid is very negligible. Thus, based on the results obtained from the grid independence study, the medium grid size was chosen for further work involving numerical computations, taking advantage of the accuracy of the refinement process, data storage, and computational time.

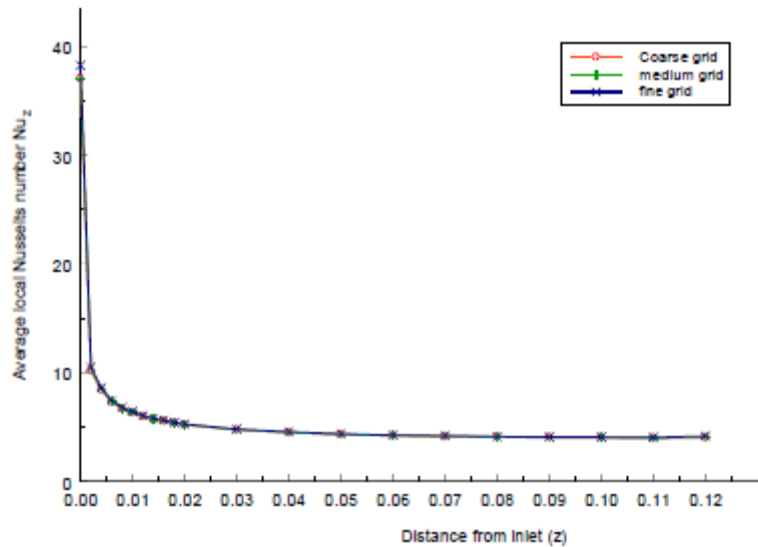


Fig 2 Average local Nusselt number v/s channel length for three grid sizes

3. RESULTS AND DISCUSSION :

3.1. Conventional Unfinned Channel :

The fully developed average local Nusselt numbers for the present study was obtained as 4.05 and from the literature, this value was found to be 3.676. The computational error in the Nusselts number was thus around 9%, which although not a large deviation, may be justified by the convergence criteria adopted. The present study adopts a convergence criteria of 10^{-6} in view of the computational time constraints, whereas from those adopted by the authors may be still lower.

3.2. Conventional Finned Square Channel : With the channel wall thickness and fin thickness held constant, the fin height ratio was suitably varied. A constant mass flow rate of 2.2×10^{-4} kg/s was given as the inlet for each case, while varying the fin height ratio. The external dimensions of the channel were also held a constant for all cases. Fig 3 shows the average local Nusselt number as a function of distance from the inlet of the channel for some typical cases considered. A larger average local Nusselt number could be seen at the entrance of the channel due to the development of the thermal boundary layer with the entrance section as the leading edge of the channel. Nusselt number converges asymptotically to a fully developed value at the outlet of the channel. At any particular channel location from the inlet, it can be seen that as the fin height increases, the average local Nusselt number values also increase. However, for a fin height ratio H^* of 0.80, the average local Nusselt numbers are lower, when compared to the case of a fin height ratio H^* of 0.60. This clearly shows that there is an optimum value that lies between fin height ratios H^* from 0.60 to 0.80. Curve fitting technique and interpolation were used to determine the optimum value of the fin height ratio, H^* . The optimum value fin height ratio H^* is found to be 0.67.

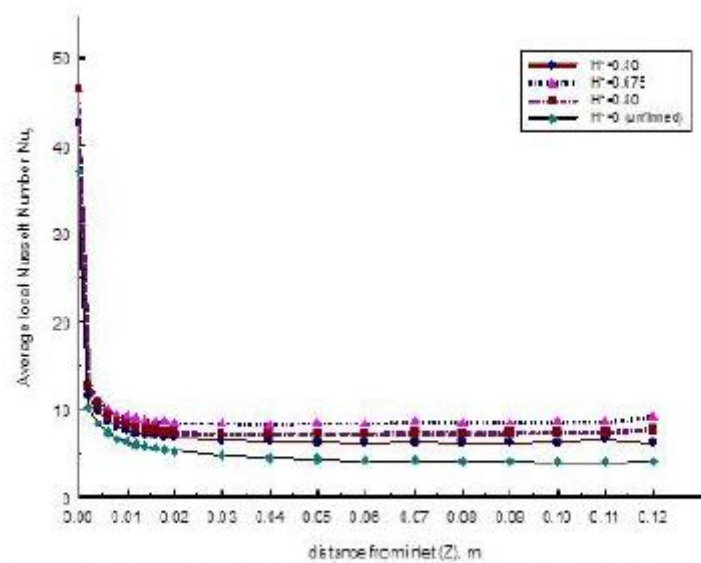


Fig. 3 Average local Nusselt number v/s distance from inlet of the microchannel (conventional finned square channels)

As stated earlier, the fully developed Nusselt number value for an unfinned square microchannel obtained from the present numerical simulation is found to be 4.05. The Nusselt number for a microchannel having internal fins and fully developed flow for an optimum fin height ratio H^* of 0.675 is found to be 9.15. This clearly shows that the Nusselt number is about 2.26 times higher for an internally finned microchannel when compared to an unfinned microchannel, thereby reinforcing the advantage of this passive heat transfer enhancement technique. Fig 4 shows the variation of average local Nusselt number as a function of the fin height ratio H^* for several cases considered in this study. This graph obviously shows the peak Nusselt number at $H^*=0.67$. For a given fluid, the thermal development length is a function of the hydraulic diameter, Prandtl number and the Reynolds number. For the same mass flow rate, in an internally finned channel, the flow reaches fully developed conditions at a shorter distance from the inlet than an unfinned channel. This is due to the fact that for the same mass flow rate in both the channels, the finned channel provides a smaller hydraulic diameter. An important factor that goes into consideration for flow through a microchannel is the pressure drop. Increase in the pressure drop increases the pumping power needed for the micropump. Fig 5 the plot of pressure drop and the average local Nusselt number in the microchannel, as a function of the fin height ratio H^* . As can be seen from graph, from the pressure drop point of view, there is no benefit in increasing the fin height ratio beyond the optimum value.

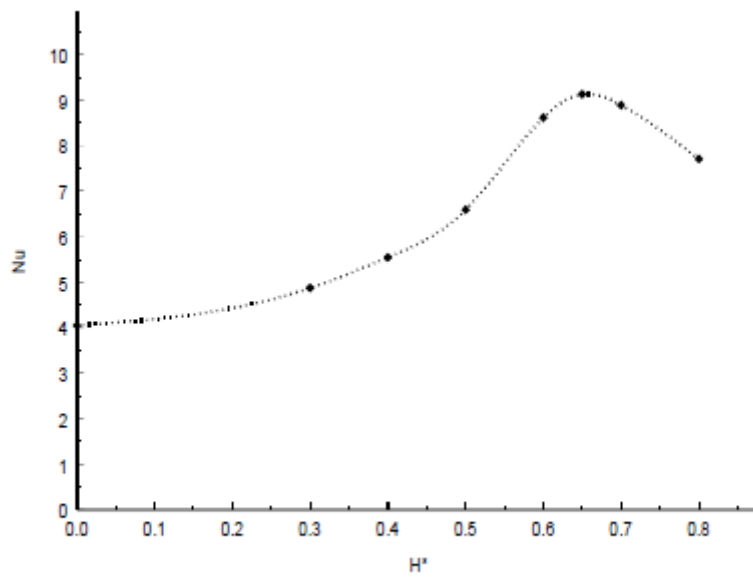


Fig 4. Average local Nusselt number v/s fin height ratio H*(conventional finned square channels)

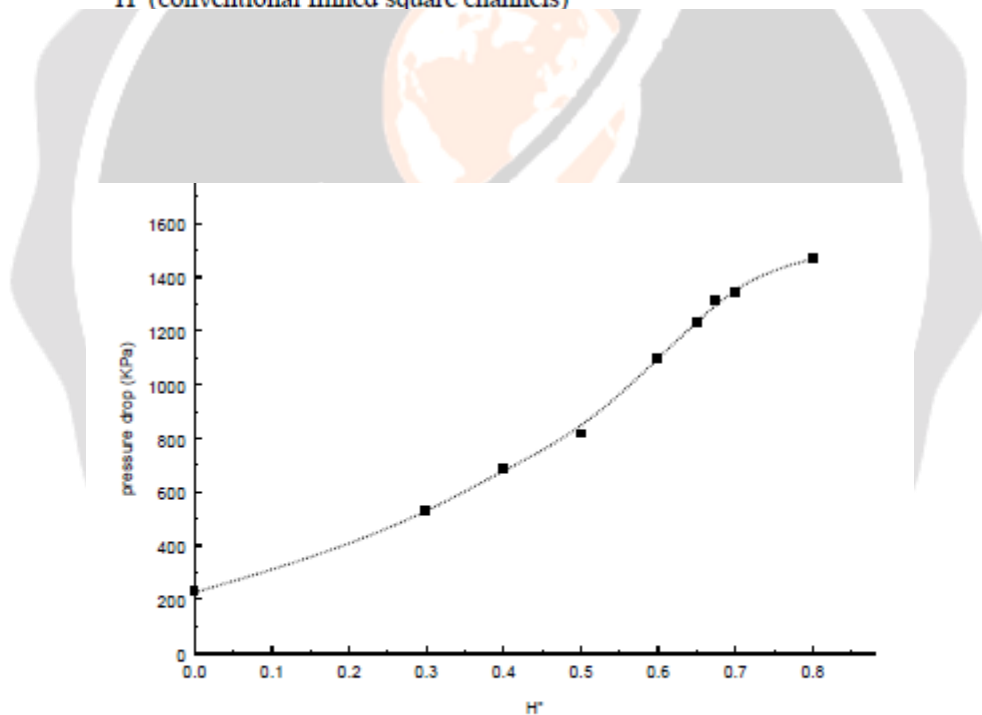


Fig 5. Pressure drop v/s fin height ratio H*

3.3 Cross Finned Square Channel :

Cross finned microchannels were introduced with the objective of improving the Nusselt number, owing to the fact that the wetted perimeter is obviously higher than that of conventional fins. The fins are erected from the corners and extend diagonally as was shown earlier in fig 1(c). As in the case of conventional finned channels, channel wall thickness and fin thickness were held constant and the fin height ratio was varied. Fig 3. shows the

average local Nusselt number as a function of distance from the inlet of the channel. A similar explanation can be given for a larger value of average local Nusselt number at the entrance section and the asymptotic convergence of the Nusselt number to a fully developed value, as in the case of conventional finned channels. It can be seen that as the fin height increases, at any particular channel location from the inlet the average local Nusselt number values also increase. However, unlike conventional finned channels, the optimum value of fin height ratio H^* is found to be 0.80, corresponding to 0.67 of the latter. Although a higher Nusselt number was expected for the cross finned channels, the optimum value is lower than that of conventional fins. Corresponding to the optimum Nusselt number of 9.15 at a fin height ratio of 0.67, the optimum value obtained here was 8.11 at a fin height ratio of 0.80. The presence of more acute corners than that of the latter and the corresponding drop in velocities at the corners may be interpreted as the reason for this unexpected lower result.

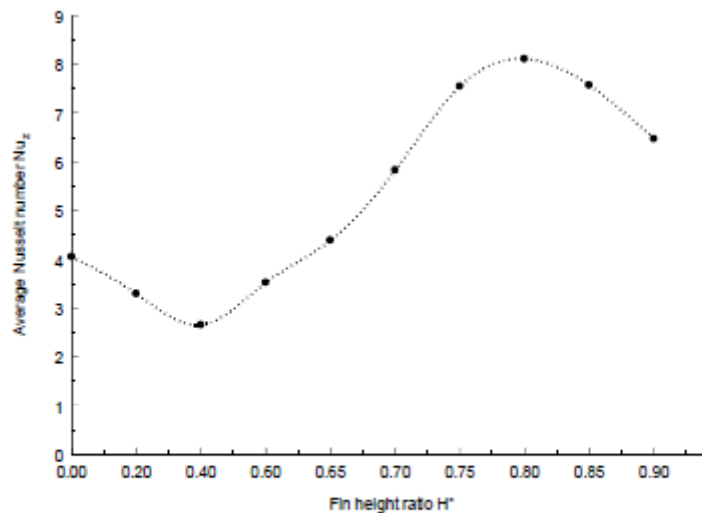


Fig 6 Average local Nusselt number v/s fin height ratio H^* (cross-finned square channels)

Fig 6 shows the variation of average local Nusselt number as a function of the fin height ratio H^* for several cases considered in this study. It can be seen that the value of average local Nusselt number first drops with increase in fin height, due to the stagnant effects of the fluid in the corners. But still higher fin heights tend to increase this as surface area of heat transfer increases. Explanations for thermal development length and pressure drop can be adopted from that of conventional channels.

3.4 Rectangular Channels With Aspect Ratio 2 :

The study was extended to rectangular channels, where the horizontal and vertical fin height ratios $H1^*$ and $H2^*$ are varied independently. Here too the external dimensions, fin and channel thickness were kept constant and the fin height ratios were varied individually, keeping the mass flow rate same at 4.4×10^{-4} kg/s. The aim of this study was to check whether the optimum fin height, if present could be found out by varying the horizontal and vertical fin height ratios equally or independently. was varied from 0.3 to 0.9. A total of 56 cases were

solved excluding that of finless rectangular channel. Fig 7 shows the average local Nusselt number as a function of distance from the inlet of the channel.

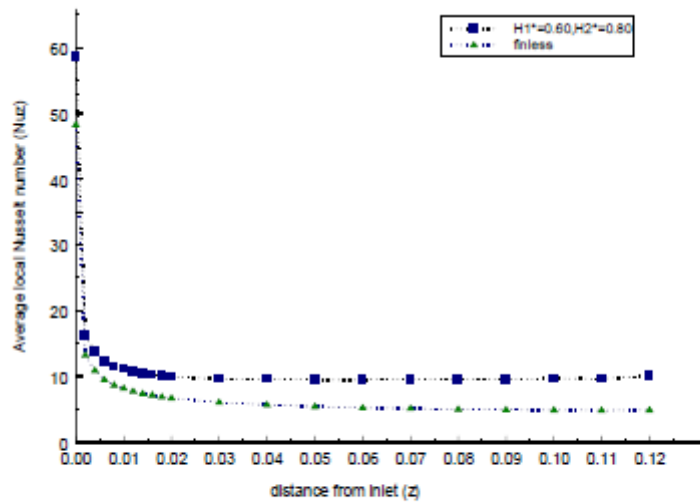


Fig 7 Average local Nusselt number v/s distance from inlet of the microchannel (conventional finned rectangular channels).



Table - Average local Nusselt number v/s fin height ratios H1* and H2*(conventional finned rectangular channels

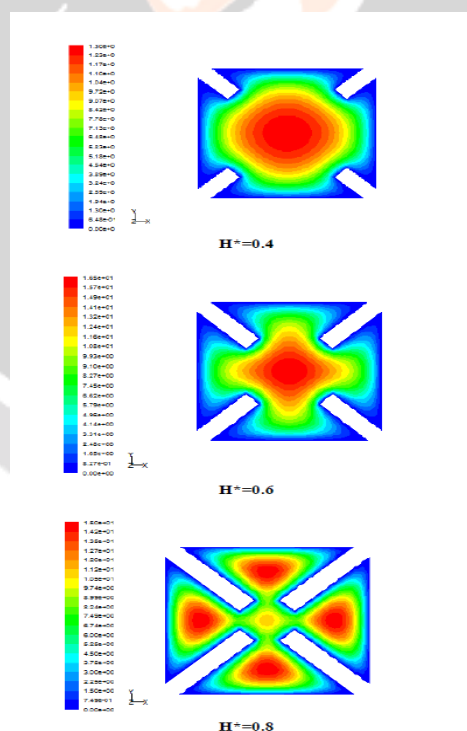
$\frac{H_1}{H_2}$	0.3	0.4	0.5	0.6	0.7	0.8	0.9
0.2	4.2424	4.3503	4.6973	5.4240	6.7585	8.7503	9.9067
0.3	4.4330	4.5932	5.0171	5.8435	7.2776	9.2131	10.0332
0.4	4.7199	4.9616	5.4975	6.4624	7.9855	9.6869	10.0093
0.5	5.0861	5.7724	6.4961	7.6872	9.2940	10.0208	9.8024
0.6	5.4731	5.9884	6.8904	8.2067	9.5855	10.0811	9.4726
0.7	5.7674	6.4453	7.5504	8.9662	9.9854	9.8462	9.1137
0.8	6.2158	6.6565	7.8767	9.2561	9.8939	9.4465	8.7922
0.9	6.1434	6.6284	7.8640	9.1516	9.5757	9.0682	8.5289

The fully developed average local Nusselt number for unfinned square microchannel was found to be 4.88. From all the values obtained, the maximum Nusselt number was found to be 10.08 for the case in which H1*=0.60 and H2*=0.80. It is thus observed that the optimum value cannot be reached by varying the horizontal and vertical fin height ratios equally. Moreover it is inferred that the effect of varying the fin height ratio of longer side (here H2*) is better than that of varying the shorter one, which is evident from the higher slope of the surface near H2* kept constant at 0.9 and H1* varied suitably. The Nusselt number thus got improved by

2.07 times from the finless value by the addition of fins in the optimum way. A table and graph showing the average local Nusselt number at exit for all the cases solved are also given. It should be noted that all this improvement in the Nusselt number was obtained at the expense of pressure drop. So it may be stated that the primary constrain for choosing the fin height of microchannels is the pumping power of the micropump employed.

3.5. Contours Of Velocity :

The contours of velocity at the exit section for different fin heights are shown in Fig 9. It is interesting to observe the migratory patterns of the velocity. In an unfinned channel, the region of maximum velocity fluid is always at the centre of the channel. When internal fins are added to the channel, the region of maximum velocity is shifted. In the case of four fins, as the fin height increases, the region of maximum velocity moves progressively, to four separate zones formed due to the presence of the fins. The existence of an optimum fin height is also very clear from figure. The figures show the development of flow pattern within the microchannel as the fin height increases. As can be seen from Fig 9, there is a significant change in the flow pattern for fin height ratios $H^* = 0.4, 0.6, 0.8$ and 0.9 . For the cases considered in this study, the best flow situation is found to occur for $H^* = 0.8$. For this case, it can also be seen that there is significant improvement in the corner flow, which helps to enhance the heat transfer in the microchannel. However for fin height above the optimum eight ratio $H^* = 0.9$, the flow pattern is not favorable for maximum heat transfer due to the stagnation of the fluid t the centre of the channel.



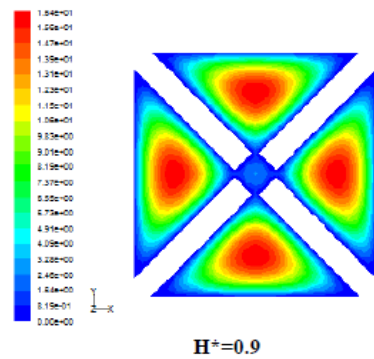


Fig 8 Velocity distribution within microchannel from centre to the corner (cross finned square channels)

For a deep insight into the phenomenon of the increase in heat transfer coefficient due to the presence of fins, the fluid velocity distribution is plotted along the diagonal extending from the center of the microchannel to one of the corners in the exit plane for the case of conventional square finned channels. This is done for H^* varying from 0 to 0.90. For finless channel, the peak velocity occurs at the center of the channel. With the increase in H^* , the velocity at center decreases and new peaks occur at the side quadrants of the channel. For the case of the channel having the optimum fin height ratio, the peak fluid velocity is found to occur at the centre region of the channel and at the side quadrants of the channel. A higher fluid velocity near the fins and at the heated section increases the convective heat transfer in the channel.

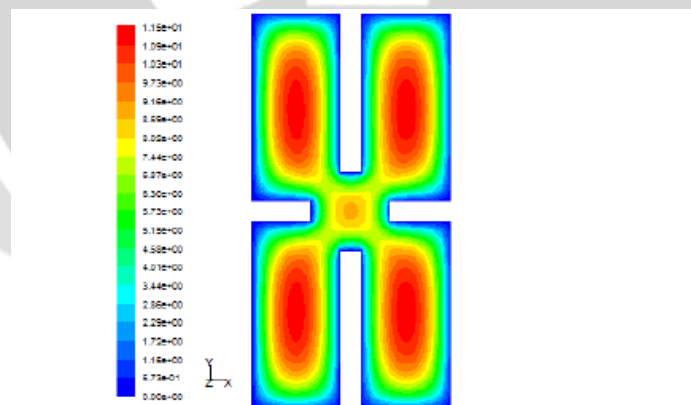


Fig .9 Velocity distribution within microchannel from centre to the corner (conventional finned rectangular channels)

Any further increase of the fin height ratio beyond the optimum value alters the flow across the centre of the channel, and the fin tip would not be effective in contributing to the convective heat transfer process that occurs within the channel. Similar interpretation can be done in case of cross finned channels also. Instead of diagonal lines, straight lines are drawn at the exit section. Velocity variation is plotted along its length. It is maximum at the center of channel and comes down to 0 at the walls. With the introduction of fins diagonally, redistribution takes place and new peaks are formed. The optimum is the case when all the peaks of fluid velocity are of

similar magnitude, which happens for $H^*=0.8$. Diagonal line at the exit is drawn again for rectangular channels where the velocity is plotted and peaks of similar magnitude corresponds to maximum Nusselt number at $H1^*=0.60; H2^*=0.80$

3.6. Comparison With Published Results: In order to validate the modelling scheme, the unfinned channel results of Ramesh and Chandratilleke [13] were compared with a case of an unfinned channel modelled in the present study. The fully developed average local Nusselt numbers for both the cases were compared. For the present study, this value was obtained as 4.05 and from the literature, this value was found to be 3.676. The computational error in the Nusselts number was thus around 9%, which although not a large deviation, may be justified by the convergence criteria adopted. The present study adopts a convergence criteria of 10^{-6} in view of the computational time constraints, whereas from those adopted by the authors may be still lower. Moreover, the thermo-physical properties were assumed to be temperature dependent. The scheme adopted by the authors is unavailable.

4. CONCLUSION :

Based on this numerical study, it was concluded that internal fins in a microchannel have the potential to provide heat transfer augmentation. The work done by Ramesh and Chandratilleke were validated. For a given microchannel, there is an optimum fin height that provides the best possible heat transfer and pressure drop characteristics. The optimum fin height ratio H^* for a square microchannel found in this study is 0.67. The following beneficial features are also realized in a microchannel with internal longitudinal fins as compared to an unfinned microchannel: shorter length required for the development of the thermal boundary layer, better flow mixing, steeper velocity gradient at the heated surface, increase in the surface area for heat transfer, and increase in surface heat transfer coefficient and Nusselt number. Similar studies were conducted on cross finned channels, and the optimum height ratio was found to be 0.80. The cross fin microchannels which when compared with the conventional finned microchannels failed to show any improvement of the optimum Nusselt number as expected. Moreover, the additional pressure drop and manufacturing constrains makes the conventional channels more efficient. From study of all the cases of rectangular channels it was understood that the optimum value might not be reached by varying the fin height ratios simultaneously equally. Improvement of fully developed Nusselt number by almost 2.07 times was obtained by adopting a fin height ratio of $H1^*=0.60$ by $H2^*=0.8$.

5. FUTURE SCOPE OF WORK :

Future scope may include extending the study to higher aspect ratio microchannels, and developing a general correlation for optimum fin heights with aspect ratio of the channel considered.

REFERANCES :

- [1] D.B. Tuckerman, R.F.W. Pease, "High -performance heat sinking for VLS", IEEE Electron. Dev. Lett., EDL 2 (5) (1981) 126 –129.
- [2] P.S. Lee, S.V. Garimella, D. Liu, "Investigation of heat transfer in rectangular microchannels", Int. J. Heat Mass Transfer 48 (2005) 1688 –1704.

- [3] W. Qu, I. Mudawar, “*Experimental and numerical study of pressure drop and heat transfer in a single - phase microchannel heat sink*”, Int. J. Heat Mass Transfer 45 (2002) 2549 –2565.
- [4] P.S. Lee, S.V. Garimella, “*Thermally developing flow and heat transfer in rectangular microchannels*” Int. J. Heat Mass Transfer 49 (17) (2006) 3060 –3067.
- [5] A.G. Fedorov, R. Viskanta, “*Three dimensional conjugate heat transfer in the microchannel heat sink for electronic packaging*” Int. J. Heat Mass Transfer 43 (3) (2000) 399 –415.
- [6] I. Alam, P.S. Ghoshdastidar, “*A study of heat transfer effectiveness of circular tubes with internal longitudinal fins having tapered lateral profiles*,”Int. J. Heat Mass Transfer 45 (6) (2002) 1371–1376.
- [7] Z.F. Dong, M.A. Ebdian, “*A numerical analysis of thermally developing flow in elliptical duct with internal fins*”, Int. J. Heat Fluid Flow 12 (2) (1991) 166 –172.
- [8] M.E. Steinke, S.G. Kandlikar, “*Single phase liquid friction factors in microchannels*”, Int. J. Therm. Sci. 45 (11) (2006) 1073 –1083.
- [9] Ramesh and Chandratilleke, ” *Laminar convective heat transfer in a microchannel with internal longitudinal fins*”, International Journal of Heat and Mass Transfer 49 (2006) 3060 -3067.

